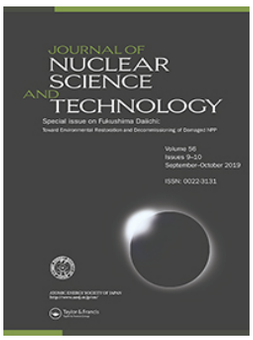

Journal of Nuclear Science and Technology

ISSN: 0022-3131 (Print) 1881-1248 (Online) Journal homepage: https://www.tandfonline.com/loi/tnst20

Radiation imaging using a compact Compton camera mounted on a crawler robot inside reactor buildings of Fukushima Daiichi Nuclear Power Station

Yuki Sato, Yuta Terasaka, Wataru Utsugi, Hiroyuki Kikuchi, Hideo Kiyooka & Tatsuo Torii

To cite this article: Yuki Sato, Yuta Terasaka, Wataru Utsugi, Hiroyuki Kikuchi, Hideo Kiyooka & Tatsuo Torii (2019) Radiation imaging using a compact Compton camera mounted on a crawler robot inside reactor buildings of Fukushima Daiichi Nuclear Power Station, Journal of Nuclear Science and Technology, 56:9-10, 801-808, DOI: 10.1080/00223131.2019.1581111

To link to this article: https://doi.org/10.1080/00223131.2019.1581111

JOURNAL OF NUCLEAR SCIENCE AND TECHNOLOGY
2019, VOL. 56, NOS. 9–10, 801–808
https://doi.org/10.1080/00223131.2019.1581111

RAPID COMMUNICATION

OPEN ACCESS Check for updates

Radiation imaging using a compact Compton camera mounted on a crawler robot inside reactor buildings of Fukushima Daiichi Nuclear Power Station

Yuki Sato[a], Yuta Terasaka[a], Wataru Utsugi[b], Hiroyuki Kikuchi[b], Hideo Kiyooka[b] and Tatsuo Torii[a]

[a]Collaborative Laboratories for Advanced Decommissioning Science, Japan Atomic Energy Agency, Fukushima, Japan; [b]Fukushima Daiichi Decontamination and Decommissioning Engineering Company, Tokyo Electric Power Company Holdings, Inc., Fukushima, Japan

ABSTRACT

The Fukushima Daiichi Nuclear Power Station (FDNPS), operated by Tokyo Electric Power Company Holdings, Inc., went into meltdown in the aftermath of a large tsunami caused by the Great East Japan Earthquake of 11 March 2011. Measurement of radiation distribution inside the FDNPS buildings is indispensable to execute decommissioning tasks in the reactor buildings. We conducted a radiation imaging experiment inside the reactor building of Unit 1 of FDNPS by using a compact Compton camera mounted on a crawler robot and remotely visualized gamma-rays streaming from deep inside the reactor building. Moreover, we drew a radiation image obtained using the Compton camera onto the three-dimensional (3-D) structural model of the experimental environment created using photogrammetry. In addition, the 3-D model of the real working environment, including the radiation image, was imported into the virtual space of the virtual reality system. These visualization techniques help workers recognize radioactive contamination easily and decrease their own exposure to radiation because the contamination cannot be observed with the naked eye.

ARTICLE HISTORY
Received 17 October 2018
Accepted 6 February 2019

KEYWORDS
Radiation imaging; remote technology; system integration; photogrammetry; virtual reality; Fukushima Daiichi Nuclear Power Station; decommissioning

1. Introduction

A large amount of radioactive substances was spread over a large area as a result of the Fukushima Daiichi Nuclear Power Station (FDNPS) accident that occurred owing to a large tsunami caused by the Great East Japan Earthquake on 11 March 2011. Decommissioning operations inside and outside the reactor buildings, including the decontamination of a large amount of radioactive substances, are underway.

Drawing a radiation distribution map that indicates the distribution of radioactive substances inside the reactor buildings is extremely important for radiation safety to workers and decreasing the amount of radiation exposure when performing decommissioning tasks. Such a map would help workers recognize the locations of radioactive substances in the work environment easily. In addition, the information can be used to establish detailed decontamination plans.

Inside the FDNPS site, handheld survey meters are used frequently to measure the distribution of radioactive substances. However, such measurement over a wide area is time consuming, and radiation exposure to workers during the survey is a critical issue. Moreover, local hotspots may be overlooked.

The combination of a gamma-ray imager and remote equipment is useful for remotely measuring radioactive substances over a wide area or in high dose-rate environments, such as inside the FDNPS buildings, which workers are difficult for entering. Gamma-ray imagers are powerful devices for measuring the distribution of radioactive substances over a wide area inside the field of view (FOV) of each imager. In particular, Compton cameras use the kinematics of Compton scattering to estimate the incident direction of gamma rays toward the sensor. Accordingly, shielding techniques such as a heavy collimator of a pinhole camera are unnecessary in principle. For example, hotspot detection inside the FDNPS site by using an omni-directionally sensitive Compton camera has been reported [1].

Attempts to remotely measure radioactive substances by using Compton cameras mounted on unmanned aerial vehicles, such as unmanned helicopters or multicopter-type drones, have been reported by several researchers, including our team [2–4]. Radiation distribution maps of the outdoor environment of the coastal area (Hamadori region) in Fukushima prefecture have been obtained.

In addition, inside the FDNPS buildings, three-dimensional (3-D) identification of the location of radioactive substances is necessary to draw a detailed radiation distribution map because the radioactive substances have spread over the ceiling, walls, and many building structures, as well as to the ground floor. In this light, we developed a method to visualize radioactive substances by superimposing

CONTACT Yuki Sato sato.yuki@jaea.go.jp Collaborative Laboratories for Advanced Decommissioning Science, Japan Atomic Energy Agency,790–1 Motooka aza Ohtsuka, Tomioka-machi, Futaba-gun, Fukushima 979–1151, Japan

images of radioactive substances on a 3-D structural model that reproduces the working environments inside the FDNPS buildings.

Previously, we conducted a radiation imaging experiment inside the turbine building of Unit 3 of the FDNPS by using a compact Compton camera and succeeded in visualizing hotspots (up to 3.5 mSv/h) [5]. In that test, lead shields with a thickness of 1 cm each were placed on five faces, except for the front side of the gamma-ray sensor, to reduce the number of gamma rays incident on the gamma-ray sensor. When the number of incident gamma rays per unit time increases, the occurrence rate of chance coincidence events also increases, and the incident direction of gamma rays toward the sensor is erroneously estimated. With the setup proposed in our previous experiment, we confirmed that the abovementioned hotspot can be detected in an environment with an air dose rate of 0.4–0.5 mSv/h. Here, the count rates were >30 and >20 kcps for scatterer and absorber, respectively.

Furthermore, we drew a 3-D radiation distribution map by integrating the hotspot images obtained using the Compton camera into point cloud data in the form of a 3-D structural model of the experimental environment acquired using a scanning laser range finder (LRF). The radiation distribution map shows the location of hotspots on a real space image of the turbine building.

In addition to the LRF, photogrammetry can be used to acquire a 3-D structural model of the working environment. Photogrammetry involves reconstruction of the 3-D models of objects or scenes by combining photographs taken from multiple angles. Moreover, we have developed a method to three-dimensionally grasp the location of radioactive substances by superimposing images of radioactive substances on a 3-D structural model of the work environment reconstructed using photogrammetry [6]. Haefner and Vetter et al. [7,8] reported a method involving superposition of an image of radioactive substances measured using a gamma-ray imager on a 3-D model of the measurement area prepared using Microsoft Kinect or other LRFs to visualize radiation sources on a 3-D real space image. The Microsoft Kinect sensor outputs RGB images and 3-D point cloud data of the scenes.

The 3-D reconstruction techniques using photographs and RGB color information make it easier to recognize the materials and types of objects, as opposed to only point cloud data when using LRF. However, the precision of 3-D reconstruction obtained with these techniques that use color information decreases in dark environments because the resolution of the color images used for reconstruction deteriorates. By contrast, the LRF system can perform measurements in dark environments because it employs laser scanning. To compensate for the disadvantages of each technology, it is desirable to promote and combine developments in both technologies from the viewpoint of application to decommissioning work at the FDNPS site.

In the present paper, we introduce a method to visualize hotspots inside the FDNPS reactor buildings by using photogrammetry. The proposed method is based on the superimposition of images of hotspots onto a 3-D structural model of the reactor building. The hotspots are detected using a compact Compton camera inside the reactor building of Unit 1 of the FDNPS. A 3-D structural model of the reactor building is reconstructed using photogrammetry; a plurality of photographs of the work environments inside the reactor building are acquired with a digital camera for reconstruction of the 3-D structural model. Because the dose rate inside the reactor building is high and workers cannot work there for extended durations, we installed the Compton camera and the digital camera on a small crawler robot and conducted hotspot detection and photography remotely.

2. Experimental setup

Figure 1 shows the experimental setup used for performing measurements inside the reactor building of Unit 1 of the FDNPS. In this test, we mounted several devices on the small crawler robot (510 Packbot, iRobot, USA). To acquire photographs (still images) for photogrammetry in dark places inside the reactor building, we installed LED lights (MG-286R, GENTOS Co., Ltd., Japan) in addition to a digital camera (DSC-RX100M3, SONY, Japan). The brightness of the LED light was set to 700 lm.

The gamma-ray sensor and the signal processing unit of the Compton camera were installed in an aluminum box and mounted on the robot, as shown in Figure 1(c). A 27-mm-thick lead shield was installed to surround the gamma-ray sensor. There was no pinhole in the shield in front of the gamma-ray sensor. Unlike pinhole cameras, with a Compton camera, it is possible to estimate the angle of incidence of gamma rays on the gamma-ray sensor from the energy deposition on the sensor and the interaction position of the sensor without using a pinhole collimator. The specifications of our Compton camera are described in detail in Refs. [3,9]. The performance of the Compton camera used for the demonstration test is also shown in Table A1 (see Appendix). Gamma-ray sensors of the Compton camera, namely, scatterer and absorber, employed a Ce-doped GAGG ($Gd_3Al_2Ga_3O_{12}$) scintillator coupled with a multipixel photon counter (MPPC; Hamamatsu Photonics K.K.) [10,11]. The time window for acquiring the coincidence events between the scatterer and the absorber was set to 200 ns. This camera was fabricated

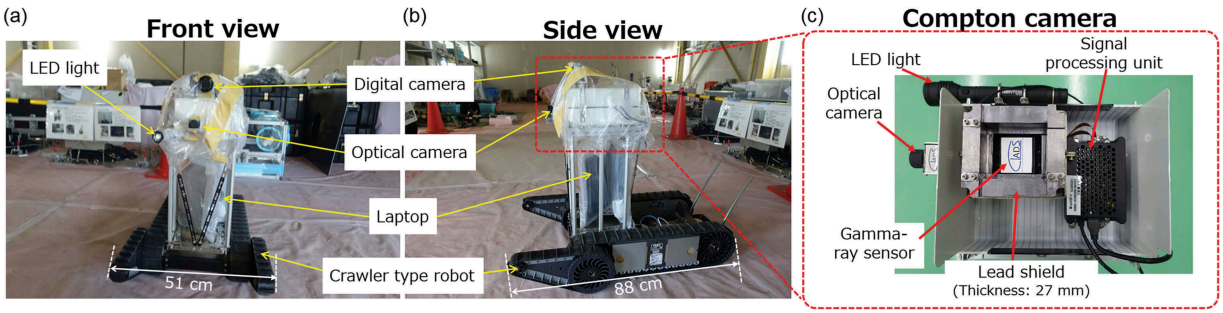

Figure 1. Photograph of experimental setup. Compton camera, digital camera, LED light, and laptop were mounted on the crawler robot. Front view and side view are shown in panels (a) and (b), respectively. Panel (c) shows the Compton camera, which is the same device as that used for hotspot detection inside the turbine building of Unit 3 of FDNPS described in Ref [5]. The lead shield on the top of the gamma-ray sensor was removed to show the insides. There is no pinhole in the shield in front of the gamma-ray sensor.

based on the technology of a handheld Compton camera jointly developed by Waseda University and Hamamatsu Photonics [12,13].

The optical camera (NM33-F, OPT Corporation, Japan) was installed outside the aluminum box, and the hotspot locations could be visualized two-dimensionally by superimposing the reconstructed image of the hotspots on the acquired optical image obtained using the optical camera (see Figure 3). In addition, the signal processing unit and the optical camera of the Compton camera were connected via USB to the laptop (CF-SZ5, Panasonic, Japan) mounted on the robot. Electric power was supplied to the Compton camera from the laptop. Operation of the Compton camera via the laptop and maneuvering of the crawler robot were carried out remotely from the Main Anti-Earthquake Building because of a high dose rate of >1 mSv/h inside the reactor building; a Wi-Fi router located inside the carry-in entrance of the reactor building was wired to the network of the Main Anti-Earthquake Building.

3. Drawing hotspot image on 3-D structural model of inside the reactor building of Unit 1

We attempted to draw an image of the hotspots on the 3-D structural model of the inside the reactor building of Unit 1 of the FDNPS. Figure 2 schematically shows the top view of the experimental environment. The crawler robot entered from the carry-in entrance of the reactor building and proceeded straight ahead. A shielding was located ahead of the direction of motion of the robot to prevent effects of the radiation from deep inside the reactor building, as shown in Figure 2.

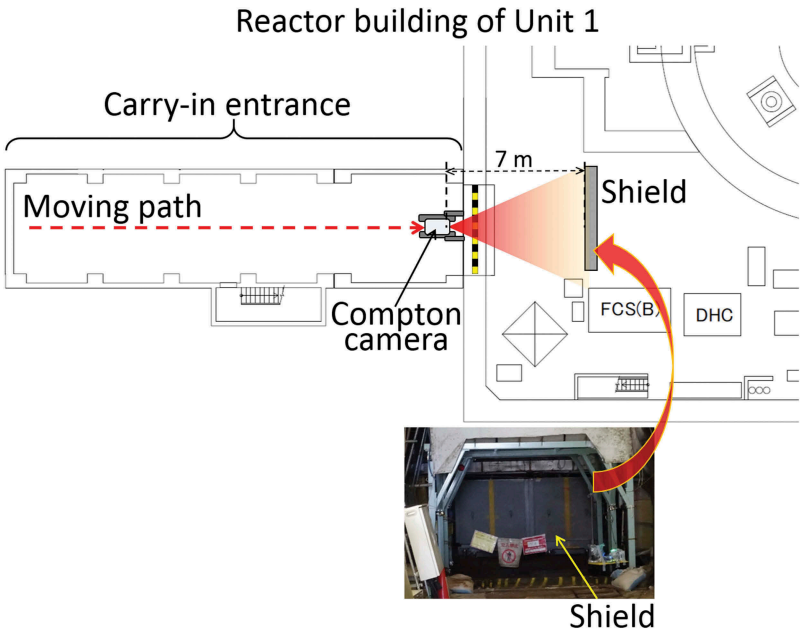

Figure 2. Schematic of top view of experimental environment inside reactor building of Unit 1 of FDNPS. Dashed arrow shows the direction of motion of the crawler robot. A shield is located ahead of the direction of motion of the robot. Radiation measurement using the Compton camera was carried out from a point about 7 m away from the shield.

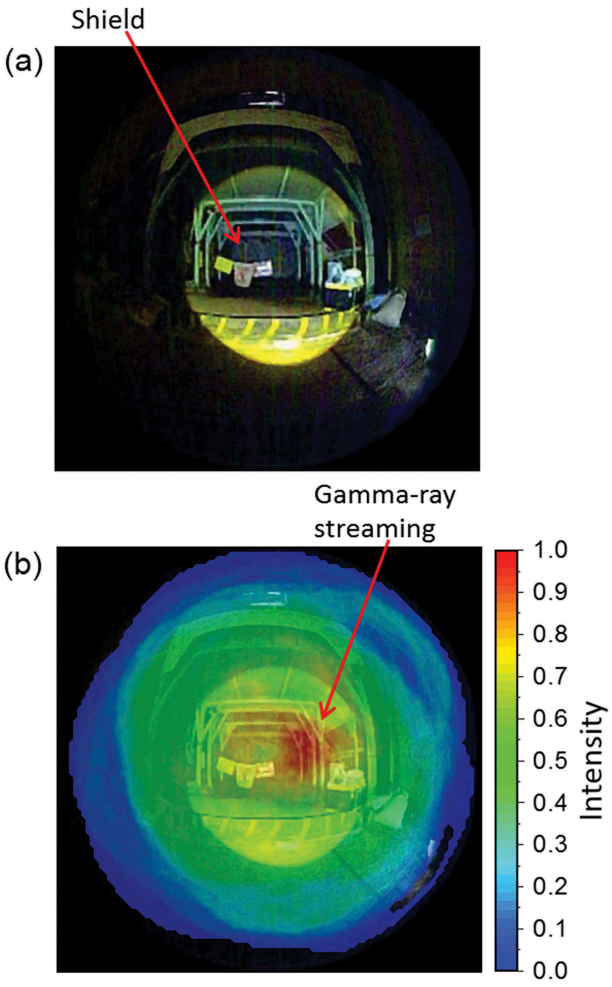

Figure 3. Radiation imaging measurement using Compton camera. Panels (a) and (b) show the photographs captured using the optical camera of the Compton camera and the reconstructed radiation image. The measurement time was 26 s. Gamma-ray streaming was detected at the right end of the shield. The color bar represents the degree of overlap of the Compton cones and dose not corresponds to the dose rate.

First, we detected a hotspot remotely by using the Compton camera. The measurement date was 19 March 2018. Figure 3(a) shows the measurement environment recorded using the optical camera of the Compton camera. The distance between the Compton camera and the shielding was approximately 7 m (see Figure 2). The dose rate at the installation position of the Compton camera was measured by survey meter in advance, and it was approximately 5 mSv/h.

Figure 3(b) shows the measurement results obtained via radiation imaging by using the Compton camera. In particular, the figure illustrates a radiation image created by drawing the Compton cones simply superimposed on a two-dimensional (2-D) photograph captured by the optical camera. The intensity described by the color bars represents the degree of overlap of the Compton cones. In accordance with the principle of the Compton camera, we can find the hotspot at the intersection point of the Compton cones [9]. The count rates in the scatterer and the absorber of the gamma-ray sensor were 5 and 7 kcps, respectively. We have succeeded in detecting hotspots locally existed inside the turbine building of Unit 3 in the case of the count rates of >30 and >20 kcps for scatterer and absorber, respectively. From the viewpoint of the count rate counted this time, it can be argued that the ability to visualize locally existing hotspots has not been lost.

The result shows that the image of the hotspot appears at the right end of the shielding. At this end, a Drywell Humidity Control (DHC) is installed at the far side of the right end of the shielding, as shown in Figure 2. TEPCO's preliminary survey reported air dose rates >100 mSv/h near the DHC [14]. The image of the detected hotspot is expected to have a large contribution from gamma rays emitted from the vicinity of the DHC (Tokyo Electric Power Company Holdings, Inc., private communication). On the other hand, gamma rays flying from areas deeper than the DHC are detected naturally. In addition, radioactive substances spread with a certain distribution as a matter of course, and the flying direction of gamma rays also spreads; hence, the imaging result is not represented at one point locally, unlike measuring the point source as shown in Figure 4.

In this measurement, the measurement time for image reconstruction was 26 s. The event data used for image reconstruction were selected to observe the contamination due to ^{137}Cs, which emits 662-keV gamma rays, because the main source of radioactive contamination inside the FDNPS buildings is ^{137}Cs. Figure 5 is the energy spectra of gamma rays inside the measurement environment acquired by the gamma-ray sensor of the Compton camera. An energy peak due to a gamma-ray of 662 keV emitted from ^{137}Cs was observed. The selected energies for image reconstruction were set to 625 keV $\leq E_s + E_a \leq$ 725 keV and 10 keV $\leq E_s \leq$ 165 keV, where E_s and E_a denote energy deposition in

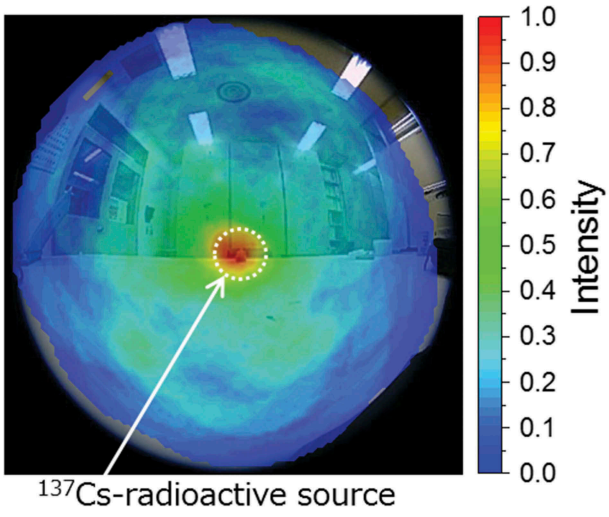

Figure 4. Reconstructed radiation image of ^{137}Cs-radioactive point source obtained using the compact Compton camera.

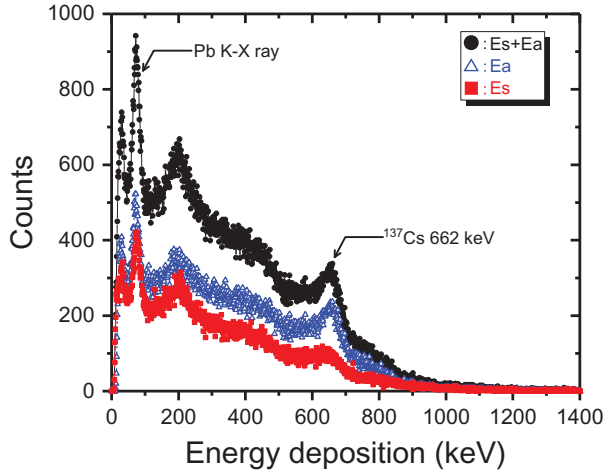

Figure 5. Energy spectra of a gamma ray in the measurement environment obtained with the Compton camera. The horizontal axis is the energy depositions in the scatterer (solid squares) and the absorber (open triangles) of the gamma-ray sensor. Sum of the energy depositions in the scatterer and the absorber of the gamma-ray sensor is also shown (solid circles). Energy peaks due to a gamma ray of 662 keV emitted from ^{137}Cs were observed. Characteristic X-ray peaks caused by the lead used for shielding of the gamma-ray sensor were also observed around 74 keV. The peaks existing around 30 keV were due to the dark noise of MPPC.

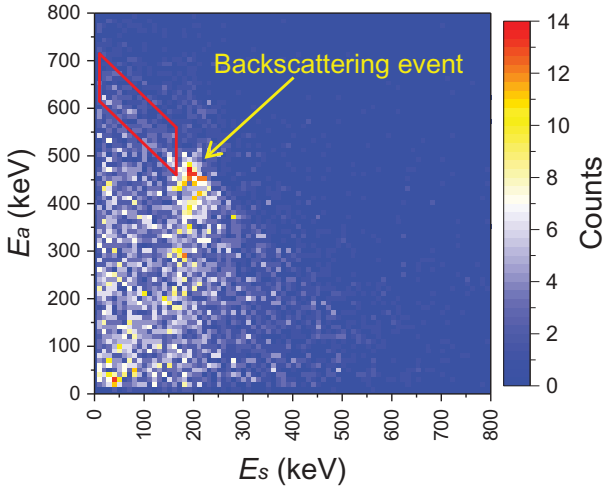

Figure 6. 2-D plot of the energy depositions in the scatterer (E_s) and the absorber (E_a). The area of the event selection is enclosed in a red line. The high-intensity region (E_s ~200 keV and E_a ~450 keV) reflects backscattering events; gamma rays are first scattered in the absorber and then absorbed in the scatterer.

the scatterer and absorber, respectively. Characteristic X-ray peaks caused by the lead used for shielding of the gamma-ray sensor were also observed around 74 keV. The peaks existing around 30 keV were due to the dark noise of MPPC. The tail of the higher energy above about 700 keV seems to be formed by combining the pile-up events and the gamma rays emitted from ^{134}Cs. The contributions of 1038, 1167, and 1365 keV gamma rays emitted from ^{134}Cs to the energy tail were suspected. In addition, the energy peak due to gamma rays (796 and 804 keV) emitted from ^{134}Cs could not be observed because the gamma-ray sensor did not have an energy resolution capable of separating energy peaks due to gamma rays emitted from ^{134}Cs and ^{137}Cs.

The 2-D plot of the energy depositions in the scatterer and the absorber is also shown in Figure 6. The area of the event selection is enclosed in a red line. The backscattering events was observed at a high intensity (E_s ~200 keV and E_a ~450 keV) compared with the surroundings, but it was outside the event selection area. No significant increase in the number of events inside the selection area was observed around the energy depositions of 30 and 74 keV in the scatterer.

It is expected that gamma rays emitted from ^{134}Cs were mixed in the above energy setting for event selection. Here, measuring the abundance ratio of ^{134}Cs and ^{137}Cs in the measurement environment is important for estimating how much gamma rays emitted from each nuclide contribute to image reconstruction. It was reported that the energy peaks of ^{134}Cs and ^{137}Cs were separated and identified inside the building of the FDNPS using a Cadmium Zinc Telluride detector [15]. By using the abundance ratio of ^{134}Cs and ^{137}Cs in the test environment measured with such a high-energy resolution detector and considering the value of the energy resolution of the gamma-ray sensor of the Compton camera, it would be possible to estimate the contribution of ^{134}Cs-gamma rays to image reconstruction.

Next, we introduce reconstruction of the 3-D structural model of the measurement area by using photogrammetry. We used two different resolutions in the photograph. In this instance, the video in which the robot moves was acquired using the digital camera. Still images were extracted from this video, and the pixel size and the resolution of the images were 640 × 480 and 96 dpi, respectively. The other image was obtained using the same digital camera as a still image in a field survey in advance. The pixel size and the resolution of the image were 2736 × 1824 and 350 dpi, respectively. The number of such images used in photogrammetry was about 230 and 10, respectively. The color depth of all images was 24 bit.

The 3-D structural model was reconstructed using the photogrammetry software PhotoScan (PhotoScan, Agisoft LLC, Russia), and details of the 3-D reconstruction procedure are given in the cited documents [16,17]. Here we simply describe the procedure of 3-D reconstruction.

First, photogrammetry software extracts the feature points from each still image. The feature points are determined by edge and the corner detection of the object in the image. Feature point matching is performed to estimate the points that correspond to each other in a pair of images. Next, the camera position at which each photograph was taken is

estimated using the common feature points, and simultaneously, the positions of the common feature points are determined three-dimensionally by using the principle of triangulation. Then, 3-D point cloud data are generated, as shown in Figure 7(a). Unlike general triangulation, this method does not need to measure the positional relationship of each measurement point, i.e. the photographing point. It should also be noted that the position where the still images were taken and the position where the gamma-ray imaging was performed are different. Here, to reproduce the texture of the environment, a mesh is formed on the point cloud data, and images of the environment are projected, as shown in Figure 7(b).

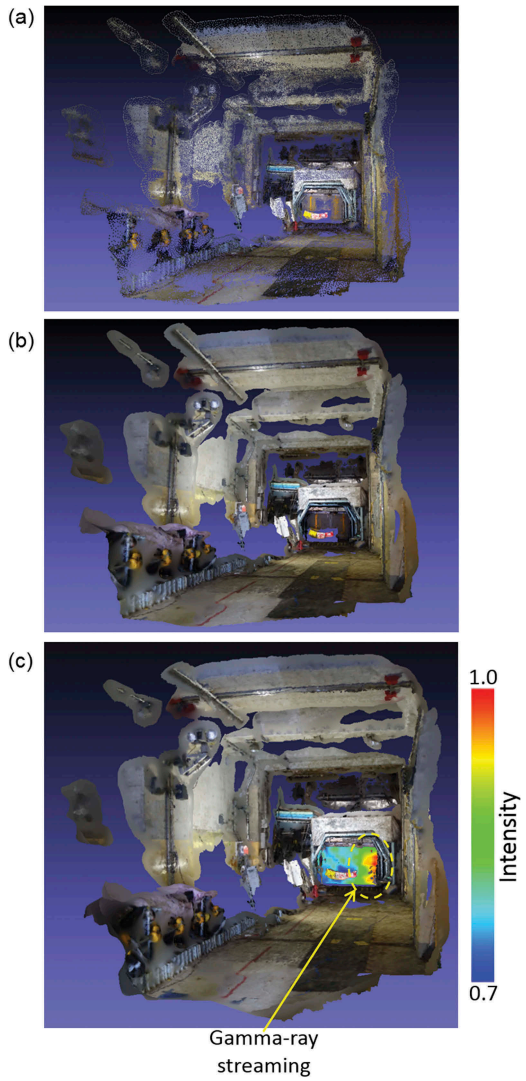

Figure 7. 3-D structural model of measurement area created using photogrammetry. Panels (a) and (b) show the point cloud data and the texture model, respectively. In panel (c), an image of the hotspot measured using the Compton camera is drawn on the 3-D texture model.

Finally, the image of the hotspot is superimposed on the surface of the shielding in the 3-D structural model, as shown in Figure 7(c). By using this 3-D model, workers can grasp the location of a hotspot in an actual working environment at a glance.

In addition to these techniques, we are developing technology to apply the above radiation distribution map to virtual reality (VR). Previously, we fabricated a VR system that displays not only the 3-D structural model of a real space but also images of radioactive substances. Details of the construction of the VR system are given in Ref. [18]. The game engine Unity 5.6 was used to construct the VR system [19]. We imported the above 3-D model containing the image of the hotspot into the VR system. Figure 8 shows a 3-D stereo view of inside of the reactor building created using Unity. The developed VR system can be accessed using a smartphone and a cardboard goggle that uses binocular lenses. Users can set the smartphone inside the cardboard goggle and look at it to locate hotspots in virtual space. Users can experience the head tracking system by using the gyro sensor and accelerometer built into the smart phone. This VR system can help easily experience the inside of the reactor buildings of FDNPS, including images of the hotspot. We believe that this system will be useful for preliminary training of workers and for recognizing radioactive hotspots during decommissioning of the work environment. It is extremely important to accurately predict the location of radioactive contamination beforehand because the working time is limited owing to radiation exposure to workers.

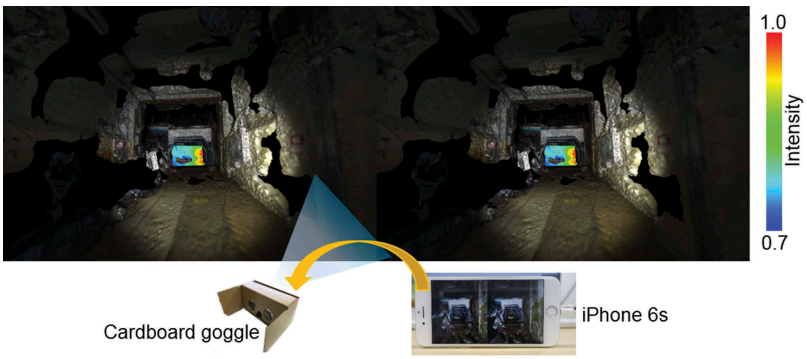

Figure 8. 3-D stereo view of image of radioactive hotspot superimposed on 3-D structural model of inside of reactor building of Unit 1 of the FDNPS.

4. Conclusion

We conducted a radiation imaging experiment inside the reactor building of Unit 1 of FDNPS by using a compact Compton camera mounted on a crawler robot and succeeded in remotely visualizing hotspots due to the gamma rays streaming from deep inside the reactor building. Moreover, we drew the hotspot images obtained using the Compton camera into the 3-D structural model of the measurement area created using photogrammetry. A 3-D model of the real working environment, which displays the hotspot image, was imported into the virtual space of the VR system. By using the VR system, before workers enter an actual work site, they can look around the inside of the working environment and get a feel for the situation, as well as grasp the location of highly contaminated equipment or rubble. Especially, because the dose rate inside the reactor building is high, grasping the location of the hotspot in advance can help with risk prediction and radiation dose reduction. The display of hotspots in the 3-D structural model that reproduces the real environment can help improve the efficiency of decommissioning work inside the reactor buildings of FDNPS.

Incidentally, the environment measured in this experiment was a straight road; the robot simply proceeded straight ahead. In environments where many objects such as equipment and rubble are scattered, a robot equipped with a Compton camera would need to accurately estimate its own location and posture. Without this information, the position and the direction for drawing Compton cones cannot be determined. We are currently developing a system incorporating self-location recognition and posture capturing using a 3-D-Lidar sensor, which would enable more extensive measurements inside the reactor buildings.

In the future, we plan to estimate radioactivity of radioactive substances using a Compton camera to calculate the dose rate for a working area. To achieve this, correction for different distances toward radioactive substances would be necessary. Even if several radioactive substances inside the FOV of a Compton camera have the same radioactivity level, the number of gamma rays detected on the Compton camera decreases with the increasing distance toward the radioactive substances. The intensities of reconstructed images of the color contour map also become weak. This phenomenon is not limited to Compton cameras; it is a common problem for all gamma-ray imagers. It is desirable to use a LRF such as a 3-D-Lidar sensor to measure the distance toward the measurement object. For the experiments reported in this paper, it would be effective to use the simultaneous localization and mapping (SLAM) system using a 3-D-Lidar sensor for taking measurements in the deep part of the reactor building. In particular, the SLAM system would enable simultaneous self-position and posture estimation in addition to the 3-D distance measurement of the measurement environment.

On the other hand, there are further problems with estimating radioactivity of a radioactive substance using a Compton camera. A weakness of the Compton camera is that it draws a circular arc (a part of a Compton cone) in a virtual space where radioactive substances do not actually exist. To reduce the impact of this feature, a method for reconstructing an image using a Compton cone having a small radius (meaning a small scattering angle of gamma rays at a scatterer) is conceivable. Moreover, it is important to correct the overlap of the FOV from each viewpoint in the measurements from multiple viewpoints using the Compton camera. When a radioactive substance is measured redundantly from multiple viewpoints, the intensity of the reconstructed image is naturally increased. We intend to measure the measurement time in each FOV one by one and use it to correct the reconstructed intensity in the redundantly measured area. To solve these problems, quantitative evaluation of radioactivity of radioactive substances scattered in the working environment inside the reactor buildings of the FDNPS will be carried out in the future.

Acknowledgments

The authors wish to acknowledge T. Hanari, Y. Tanifuji, and H. Usami of CLADS (Collaborative Laboratories for Advanced Decommissioning Science) of JAEA for supporting the experiment inside the reactor building of Unit 1 of the FDNPS. The authors also wish to acknowledge engineers of ATOX Co., Ltd. for operation of the crawler robot, K. Minemoto of Visible Information Center, Inc. for supporting the development of the 3-D reconstruction of the radiation image, and Prof. J. Kataoka and A. Kishimoto of Waseda University, S. Nakamura and M. Hirayanagi of Hamamatsu Photonics K.K. for development of base technologies of the compact Compton camera. In addition, the authors wish to acknowledge the researchers of the JAEA Oarai Research & Development for measurement of the ^{137}Cs-point source. This research was partly supported by a grant-in-aid under the Fukushima innovation coast initiative.

Disclosure statement

No potential conflict of interest was reported by the authors.

Funding

This work was partly supported by the Fukushima innovation coast initiative.

References

[1] Katagiri H, Satoh W, Enomoto R, et al. Development of an all-sky gamma-ray Compton camera based on scintillators for high-dose environments. J Nucl Sci Technol. 2018;55:1172–1179.

[2] Jiang J, Shimazoe K, Nakamura Y, et al. A proto-type of aerial radiation monitoring system using an unmanned helicopter mounting a GAGG scintillator Compton camera. J Nucl Sci Technol. 2016;53:1067–1075.

[3] Sato Y, Ozawa S, Terasaka Y, et al. Remote radiation imaging system using a compact gamma-ray imager mounted on a multicopter drone. J Nucl Sci Technol. 2018;55:90–96.

[4] Mochizuki S, Kataoka J, Tagawa L, et al. First demonstration of aerial gamma-ray imaging using drone for prompt radiation survey in Fukushima. JINST. 2017;12:P11014.

[5] Sato Y, Tanifuji Y, Terasaka Y, et al. Radiation imaging using a compact Compton camera inside the Fukushima Daiichi Nuclear Power Station building. J Nucl Sci Technol. 2018;55:965–970.

[6] Sato Y, Ozawa S, Tanifuji Y, et al. A three-dimensional radiation image display on a real space image created via photogrammetry. JINST. 2018;13:P03001.

[7] Haefner A, Barnowski R, Luke P, et al. Handheld real-time volumetric 3-D gamma-ray imaging. Nucl Instrum Methods A. 2017;857:42–49.

[8] Vetter K, Barnowksi R, Haefner A, et al. Gamma-Ray imaging for nuclear security and safety: towards 3-D gamma-ray vision. Nucl Instrum Methods A. 2018;878:159–168.

[9] Sato Y, Terasaka Y, Ozawa S, et al. Development of compact Compton camera for 3D image reconstruction of radioactive contamination. JINST. 2017;12:C11007.

[10] Iwanowska J, Swiderski L, Szczesniak T, et al. Performance of cerium-doped $Gd_3Al_2Ga_3O_{12}$ (GAGG:Ce) scintillator in gamma-ray spectrometry. Nucl Instrum Methods A. 2013;712:34–40.

[11] Hamamatsu Photonics KK. Opto-semiconductor handbook, Hamamatsu, Japan: hamamatsu Photonics K.K. In: Solid state division. 2014. Chapter 3.

[12] Kataoka J, Kishimoto A, Nishiyama T, et al. Handy Compton camera using 3D position-sensitive scintillators coupled with large-area monolithic MPPC arrays. Nucl Instrum Methods A. 2013;732:403–407.

[13] Kishimoto A, Kataoka J, Nishiyama T, et al. Performance and field tests of a handheld Compton camera using 3-D position sensitive scintillators coupled to multi-pixel photon counter arrays. JINST. 2014;9:P11025.

[14] Mizokami S Estimation of current status inside RPV and PCV at Fukushima daiichi NPS. The 2nd International Forum on the Decommissioning of the Fukushima Daiichi Nuclear Power Station; 2017 July 3; Iwaki, Japan. http://ndf-forum.com/2nd/en/program/day2.html.

[15] Mukaida N, Hayashi K, Okada K, et al. Gamma-ray spectra and dose measurement results on the reactor building refueling floor of Fukushima Daiichi Nuclear Power Station Unit 3. Paper presented at: Fall Meeting of Atomic Energy Society of Japan, Sept. 7–9, 2016 Kurume (Japan) [in Japanese].

[16] Agisoft PhotoScan, http://www.agisoft.com. [accessed 17 October 2018]

[17] Lowe DG. Distinctive image features from scale-invariant keypoints, Int. J Comput Vision. 2004;60:91–110.

[18] Sato Y, Terasaka Y, Ozawa S, et al. A 3D radiation image display on a simple virtual reality system created using a game development platform. JINST. 2018;13:T08011.

[19] Unity. https://unity3d.com. [accessed 17 October 2018]

Appendix

Table A1. Performance of the Compton camera used for the demonstration test.

	Performance	Notes
Time required for hotspot imaging (There is no shield in front of the gamma-ray sensor)	Few minutes	The dose rate of the hotspot was about 60 μSv/h, and the distance between the Compton camera and the hotspot was 2 m.
	Several tens of seconds	The dose rate of the hotspot was about 3.5 mSv/h, and the distance between the Compton camera and the hotspot was 2.7 m.
Operable dose rate environment	Up to 150 μSv/h	No shield for the gamma-ray sensor.
	Up to 0.5 mSv/h	Lead shield with a thickness of 1 cm was installed at the top, bottom, left, right, and back of the gamma-ray sensor.
Measurable field of view	Up to ±70°	^{137}Cs-checking source (point source)
Angular resolution	Less than 20°	Two hotspots with several tens of μSv/h close to 20° can be separated.